17th World Conference on Earthquake Engineering, 17WCEE
Sendai, Japan - September 13th to 18th 2020

UNCERTAINTY OF SEISMIC LOSS ESTIMATION DUE TO VARIABILITY IN THE GROUND MOTION GROUP SIZE AND DIRECTION

X. Romão[(1)], D. Skoulidou[(2)]

[(1)] *Assistant Professor, University of Porto, xnr@fe.up.pt*
[(2)] *PhD candidate, University of Porto, dskoulidou@fe.up.pt*

Abstract

Extensive damage of the existing building stock and subsequent economical losses due to past earthquakes have urged researchers to focus their studies on the vulnerability quantification of the existing building stock as well as on ways to mitigate the expected losses in future seismic events. Among the loss assessment methodologies that have been developed for this purpose, the uncertainty of all important contributing factors and its propagation to the final loss result have been greatly acknowledged. When analytical procedures using dynamic analysis are applied, the uncertainty associated to the input ground motion records resulting from the selection and scaling approach, as well as from the number of records involved, have been recognized to have a significant contribution to the overall procedure. The direction of application of the selected ground motion records, else termed the angle of seismic incidence, on the other hand, has received less attention and its effect on the final loss estimation is still under investigation. In this context, the expected loss estimates associated to the repair of earthquake-related damage in RC buildings with infilled frame systems considering the size of the group of ground motion records and the number of angles of seismic incidence involved in the analysis are analysed. Six buildings are addressed, representative of non-seismically designed structures typical of southern European practice, and economic losses are calculated applying a performance-based earthquake engineering framework. Results are presented and discussed in terms of expected losses conditional to the ground motion intensity and expected annual losses, determined by integrating the former with the seismic hazard curve of the site. The disaggregation of the expected losses is additionally performed, showing the contribution of each component to the total losses. The significant influence of the ground motion group size to the variability of the expected losses is demonstrated, unlike its effect on the central values of the expected losses, which appears to be unimportant. The effect of the angle of seismic incidence in the expected losses on the other hand is found to be trivial for most case, both with respect to their variability and central value.

Keywords: angle of seismic incidence; earthquake loss estimation; expected annual loss; ground motion group size

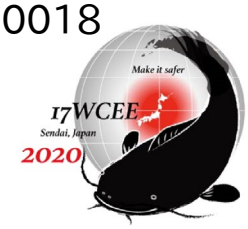

1. Introduction

The Performance-Based Earthquake Engineering framework developed by the Pacific Earthquake Engineering Research Center (PEER-PBEE) for the probabilistic assessment of the seismic performance of a building [1] allows the consideration of various sources of uncertainty. Common sources are those associated with the seismic input, expressed by the seismic hazard uncertainty [2] and the record-to-record variability [3], the structural modelling, such as the variability of geometric properties and material constitutive laws [4], the damage definitions and the economic losses [5]. It is known that accounting for such uncertainties affects the output of the different stages of the framework including the final outputs, such as the Expected Annual Loss (EAL).

The effect of various sources of uncertainties in the EAL has been examined by (e.g. [6]). Nevertheless, several aspects of the methodology still require further developments/improvements, as referred by [7]. The authors identified several shortcomings of the methodology and highlighted, in particular, the large contribution of the uncertainty related to the adopted loss model (number of damageable assemblies & distributions of repair cost) and to the building replacement cost. Furthermore, the significant influence of the indirect losses has also been pointed out by [8], demonstrating additional barriers of the current practice, as well as the need for additional data acquisition and modelling developments.

One of the variables that has been recognized to introduce a significant amount of uncertainty in the probabilistic seismic assessment of buildings is the input seismic action. The parameters related to the seismic action are associated to the Intensity Measure (IM) used for the ground motion (GM) selection, the GM group size and the direction of application of the GMs with respect to the building (i.e. the Angle of Seismic Incidence - ASI). Studies addressing the effect of the input seismic action in the probabilistic seismic assessment procedure have mostly addressed the structural analysis stages of the PEER-PBEE methodology, but relevant studies regarding its effects on the EAL are limited. The effect of the GM group size and the ASI on the variability of specific Engineering Demand Parameters (EDPs) was examined by [9], [10], where the former study also addressed the effect of the IM. The collapse risk variability was also examined with respect to the GM group size [11] and with respect to the combined effect of the GM group size and the ASI [12]. To the authors' knowledge there is only one study that addresses the effect of the GM group size and the ASI on a loss related framework and it proposes the use of 30 GMs applied in a random ASI in order to account for the uncertainty of both factors [13]. Given the lack of contributions in this area, the present study examines the effect of the ASI on the EAL of individual buildings using the PEER-PBEE framework. Since it has been shown that the effect of the GM group size is important in the estimation of the parameters associated to the various stages of the framework, the combined effect of the ASI and the GM group size on the EAL is examined. Results based on the analysis of six RC buildings aim to indicate an optimum combination of number of ASIs and GM group size for the EAL estimation.

2. Methodology

The PEER-PBEE framework is applied herein for the seismic safety assessment of six existing RC buildings to analyse the effects of the GM group size and the number of ASIs involved. The framework comprises four stages of analysis (hazard analysis, structural analysis, damage analysis and loss analysis), which are connected using the total probability theorem. The end product of the framework is the probability of exceedance of a decision variable DV that is often expressed in terms of economic losses due to the repair/replacement of the structure, casualties or downtime. In the present analyses, only the first DV is examined, namely in terms of direct economic losses. Furthermore, since the purpose of the study is to determine the effect of the input seismic action, no uncertainty is considered in the economic losses and thus the expected value of the DV, E(DV), is determined. The E(DV|IM), which represents the E(DV) conditional to the IM intensity level is given by

$$\mathrm{E}(DV \mid IM_m) = E(DV \mid NC \cap R, IM_m)P(\mathrm{NC} \cap R \mid IM_m) + E(DV \mid NC \cap D)P(\mathrm{NC} \cap D \mid IM_m) + E(DV \mid C)P(\mathrm{C} \mid IM_m) \quad (1)$$

where, NC and C stand for the no-collapse and collapse events, respectively, R stands for the repair and D for the demolition event. P denotes the cumulative distribution function. The three individual loss-related components are: $\mathrm{E}(DV|\mathrm{NC} \cap \mathrm{R}, IM_m)$, the expected loss of the building given that no collapse has occurred and the building can be repaired for the occurrence of IM_m $\mathrm{E}(DV|\mathrm{NC} \cap \mathrm{D})$, the expected loss of the building given that no collapse has occurred, but the building needs to be demolished for the occurrence of IM_m $\mathrm{E}(DV|\mathrm{C})$ the expected loss of the building when collapse occurs at IM_m. For simplicity, the expected loss corresponding to having to demolish and rebuild the building, as well as the expected loss of the collapsed building, are taken equal to the replacement cost of the building. The replacement cost is considered herein as the cost of the new building increased by a factor of 1.2 that accounts for demolition needs, the removal of debris and the fact that these operations occur during an emergency situation.

The weighting factors attributed to each cost-related component in Eq. (1) correspond to: $\mathrm{P}(\mathrm{C}|IM_m)$, the probability of collapse of the building given the IM_m, determined according to [14]. $\mathrm{P}(\mathrm{NC} \cap \mathrm{D}|IM_m)$, the probability that the building should be demolished given that no collapse has occurred at IM_m. The latter probability is defined by the residual maximum interstorey drift ratio (RISD), assuming that the limit RISD follows a lognormal distribution with median of 1.5% and a logarithmic standard deviation of 0.3 [15]. $\mathrm{P}(\mathrm{NC} \cap \mathrm{R}|IM_m)$, the probability that the building can be repaired given that no collapse has occurred at IM_m;

Finally, the expected annual value of the DV is obtained by the convolution of Eq. (1) with the annual seismic hazard curve:

$$\mathrm{E}(DV) = \sum_m E(DV \mid IM_m)\,\mathrm{p}(IM_m) \quad (2)$$

where the E(DV) corresponds to the expected annual direct economic losses in the present research, simply denoted as EAL. The results of Eqs. (1) and (2) are determined for the six buildings using bidirectional GMs in groups of size *n* ranging from 10 to 40, applied along 1 to 12 ASIs for 20 intensity levels. GM groups of size *n* equal to 40 are initially selected for each building in order to be compatible with a response spectrum that represents the seismic scenario. Subsequently, the groups of 40 records are regrouped to create GM groups of smaller sizes *n* equal to 10, 15, 20, 25, 30 and 35, according to a regrouping procedure [16], which takes into account the requirements needed to maintain the compatibility with the seismic scenario for all the new GM groups. The overall procedure leads to 100 groups for each combination of GM group size n and number of ASIs, and to an equal number of EAL values, which provides adequate data for statistical post processing.

3. Case studies

3.1 General characteristics of the buildings and modelling techniques

Six RC buildings with infilled frame systems are analysed. The selected buildings have configurations ranging from low- to mid-rise buildings with and without in-plan irregularities. The plan view of a typical storey of the 3-story irregular (3-Ir), the 4-story irregular (4-Ir) and the 5-story irregular (5-Ir) is presented in Fig. 1, along with the design details. The height of the first storey is 3.5 m and the height of all upper storeys is 3.0 m. Similarly, Fig. 2 shows the plan view of a typical storey of the 3-story regular (3-R), the 4-story regular (4-R) and the 5-story regular (5-R) building and the design details. All regular buildings have a unique storey height equal to 3.0 m. All buildings are located in Lisbon, Portugal, and are designed for gravity loads only.

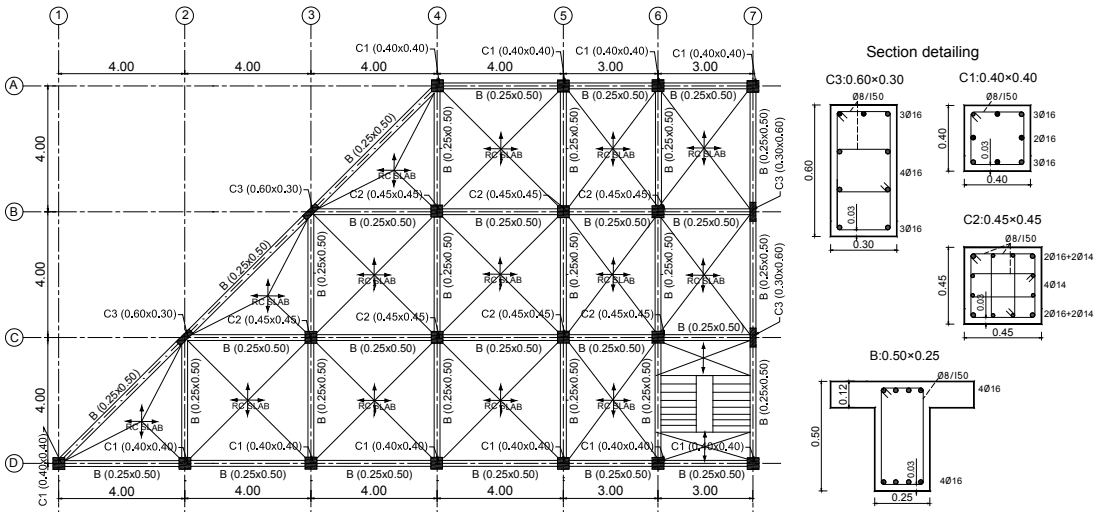

Fig. 1 - Plan view of a typical storey of the 3-Ir, 4-Ir and 5-Ir buildings and the design details (all dimensions are in m).

The buildings are analysed using three-dimensional models and a lumped plasticity approach. The computer software OpenSees [17] is used for the numerical analysis considering mean values of all material and geometrical properties. Masonry infills are considered in all peripheral frames and are modelled with a single strut active only in compression. Further information about the building material properties and modelling details can be found in [12].

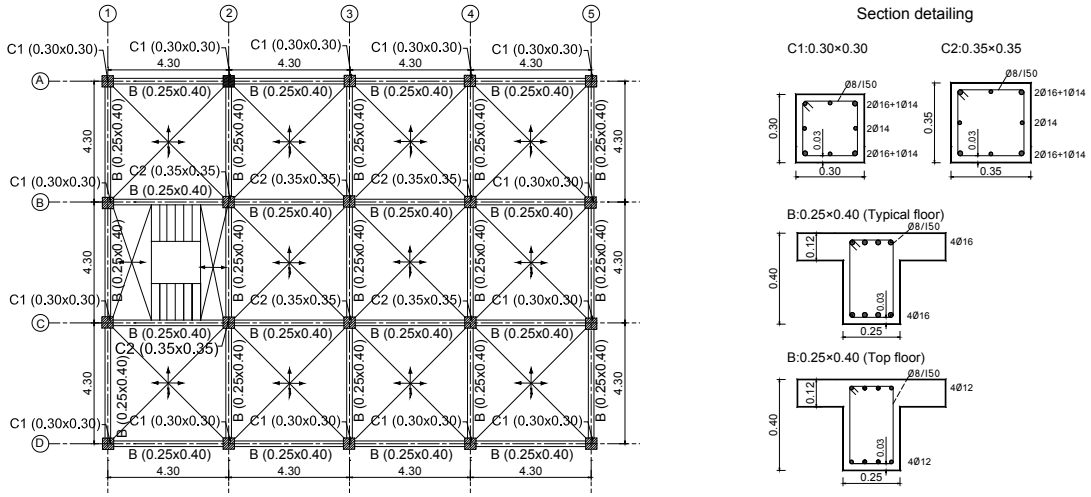

Fig. 2 - Plan view of a typical storey of the 3-R, 4-R and 5-R buildings and the design details (all dimensions are in m).

The average of the first two periods of the infilled structure and the first two periods of the bare structure T^* is determined (also shown in Table 1) to be used for the ground motion selection.

Table 1 - Average periods of the buildings

Period\Building	3-R (s)	4-R (s)	5-R (s)	3-Ir (s)	4-Ir (s)	5-Ir (s)
T^*	0.50	0.66	0.82	0.27	0.38	0.48

3.2 Identification of the damageable inventory and damage fragility parameters

In order to compute realistic loss estimations for the buildings under analysis, their architectural layouts are also developed. The building blueprints are provided in Fig. 3 for the in-plan irregular and regular buildings, in which the exact location of the non-structural damageable components are shown (i.e. stairs, infill walls, windows and doors), as well as the usage of each room:

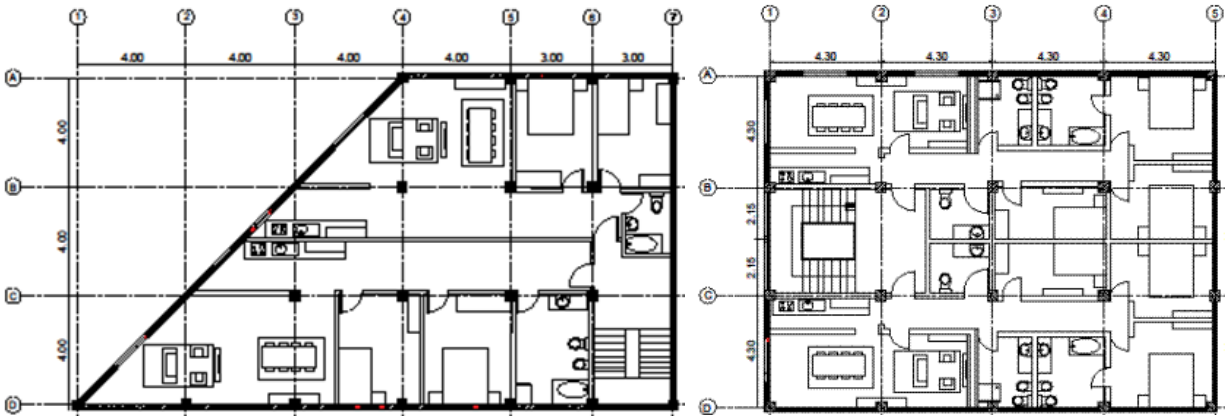

Fig. 3 – Irregular (left) and Regular (right) building blueprint (all dimensions are in m).

The buildings' inventory, comprising both structural and non-structural damageable components, is presented in Table 2 for the irregular and for the regular buildings, along with the quantities per storey. For each component, the quantities are expressed in units based on the selected method of repair (presented in the following Section). The electrical wiring and piping utilities are considered as a unity within infill walls. Regarding their position in plan, all infill walls are considered to have electrical wirings, while only infill walls of bathrooms and kitchens are considered to have piping utilities.

Table 2 - List and quantities of damageable components per storey for the irregular and regular buildings (the number in parenthesis indicates the results for the first storey of the Irregular building)

Component	Irregular Building						Regular Building					
	Unit	Quantity/ storey		Unit	Quantity/ storey		Unit	Quantity/ storey		Unit	Quantity/ storey	
Columns	ea	22		m^2	95.5 (114.6)		ea	20		m^2	65.52	
Beams	ea	36		m^2	187.53		ea	31		m^2	160.42	
Infill walls	ea	32		m^2	261.02 (320.4)	m 267.58 (325.38)	ea	39		m^2	360.2	m 367.2
Wooden doors	ea	9		m^2	15.48		ea	16		m^2	35.2	
Aluminium windows	ea	13		m^2	29.25		ea	12		m^2	27	
Suspended ceiling	m^2	192					m^2	221.88				
Stairs	ea	1		m^2	12.45 (12.88)	m 5.8 (6.2)	ea	1		m^2	17.14	m 8
Electrical Wiring	ea	32					ea	39				
Piping utilities	ea	15					ea	19				

For each damageable component, the probability of occurrence of a given damage state (DS) conditioned to a series of increasing levels of the response defined in terms of a preselected engineering demand parameter (EDP) is defined by a fragility function. These fragility functions are defined for a number of sequential DSs and are assumed to be expressed by lognormal distribution functions. The EDPs selected to express damage depend mainly on literature availability and different EDPs are selected to associate damage for the different damageable components. A list of the DSs used for all components, the associated description of the damage, the EDPs and the lognormal function parameters is given in Tables 3-6 (references used: [18],[19],[20],[21]). The damageable components presented in Table 2 that do not appear in Tables 3-6, i.e. doors, windows, electrical wiring and piping utilities, are located within the infill walls, therefore their fragility function is assumed to be equal to that of the infill they belong to.

Table 3 – Fragility and consequence function parameters for the columns and beams of the buildings

Component	Damage State	Description of Damage	Fragility Function Parameters			Consequence function parameters		
			EDP used	Median	Dispersion	Repair action	Unit	Unit Cost (€)
Column	DS1	Cracking (w>0.8mm) Initiation of yielding	Rot (rad)	0.008	0.5	Epoxy resin injection	ea	300
						Coating	m^2	39
						Paint	m^2	13.5
	DS2	Spalling	Rot (rad)	0.0175	0.5	RC jacketing (10cm)	m^3	960
						Coating	m^2	39
						Paint	m^2	13.5
	DS3	Buckling of bars	Rot (rad)	0.043	0.5	Replacement	ea	600
						Coating	m^2	39
						paint	m^2	13.5
	DS4	Element out of position	Rot (rad)	0.058	0.5	Replacement	ea	600
						Coating	m^2	39
						paint	m^2	13.5
Beams	DS1	Cracking (w>0.8mm) Initiation of yielding	Rot (rad)	0.01	0.5	Epoxy resin injection[2]	ea	300
						Coating	m^2	39
						Paint	m^2	13.5
	DS2	Spalling	Rot (rad)	0.02	0.5	RC jacketing (10cm)	m^3	1020
						Coating	m^2	39
						Paint	m^2	13.5
	DS3	Buckling of bars	Rot (rad)	0.056	0.5	Replacement	ea	700
						Coating	m^2	39
						paint	m^2	13.5
	DS4	Element out of position	Rot (rad)	0.062	0.5	Replacement	ea	700
						Coating	m^2	39
						paint	m^2	13.5

Table 4 – Fragility and consequence function parameters for the stairs of the buildings

Component	Damage State	Description of Damage	Fragility Function Parameters			Consequence function parameters		
			EDP used	Median	Dispersion	Repair action	Unit	Unit Cost (€)
Stairs	DS1	Light damage	ISD	0.01	0.4	Repair		0.30DS3
	DS2	Extensive damage	ISD	0.0175	0.4	Repair		0.50DS3
	DS3	Total collapse	ISD	0.0322	0.4	New RC stairs	ea	1100
						Coating	m^2	39
						Paint	m^2	13.5
						Covering	m^2	45
						Finishing	m^2	105
						Handrail	m	105

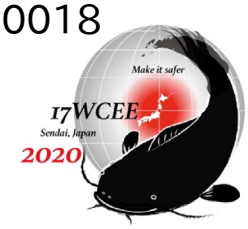

3.3 Consequence data

Each DS is associated to a method of repair and a corresponding monetary cost. The methods of repair used in the present study, as well as the corresponding costs, were selected in order to reflect up-to-date Portuguese practice. In order to achieve that, a series of meetings with practice engineers from several construction companies were performed, involving exchange of knowledge and experience. Tables 3-6 aggregate the obtained information and the data used for the loss analysis of the examined buildings. All costs include administration costs and the margin of profit, applied as a uniform amplification factor equal to 1.5. Furthermore, all costs were also amplified by a factor 2 to account for the increase in prices and costs related to displaced workers in an emergency situation. Costs do not include tax. For all repair actions related to extensive repair works or replacement of beams and columns, the cost of replacing the coating and the finishing of the area adjacent to the damaged element is also added. The respective costs were taken equal to 45 €/m^2 and 105 €/m^2. Finally, the building replacement cost is estimated based on data received from the referred Portuguese practice engineers. For low- to mid- rise RC frame buildings with masonry infills, an average price of 800€/m^2 is adopted for new buildings.

Table 5 – Fragility and consequence function parameters for the masonry infills of the buildings

Component	Damage State	Description of Damage	Fragility Function Parameters			Consequence function parameters		
			EDP used	Median	Dispersion	Repair action	Unit	Unit Cost (€)
Infills	DS1	Separation of the infill from the frame	ISD	0.00075	0.5	Repair mortar	m	9
				0.0015		Paint	m^2	13.5
				0.001		Repair wire	ea	0.20DS4
				0.0015		Repair pipes	ea	0.20DS4
	DS2	Extensive diagonal cracking (1mm<w<2mm)	ISD	0.002	0.5	Treatment of the cracked zones	m^2	27
				0. 004		Paint	m^2	13.5
				0.003		Repair wire	ea	0.20DS4
				0.004		Repair pipes	ea	0.20DS4
	DS3	In-plane or out-of-plane collapse	ISD	0.005	0.4	Demolition	m^2	27
						New wall	m^2	42
				0.01		Coating	m^2	18
						Paint	m^2	13.5
				0.0075		Replace wooden door	m^2	675
						Replace alum. window	m^2	1050
				0.01		New blinds	m^2	45
						Remove blinds	ea	81
						Repair wires	ea	0.80DS4
						Repair pipes	ea	0.8DS4
	DS4	In-plane or out-of-plane collapse	ISD	0.005	0.4	Demolition	m^2	27
						new wall	m^2	42
				0.01		Coating	m^2	18
						paint	m^2	13.5
				0.0175		replace wooden door	m^2	675
						replace alum. window	m^2	1050
				0. 0175		new blinds	m^2	45
						remove blinds	ea	81
						Repair wires	ea	285
						Repair pipes	ea	408

Table 6 – Fragility and consequence function parameters for the suspended ceilings of the buildings

Component	Damage State	Description of Damage	Fragility Function Parameters			Consequence function parameters		
			EDP used	Median	Dispersion	Repair action	Unit	Unit Cost (€)
Suspended ceiling	DS1	Light damage	PFA (g)	0.9	0.4	Repair		0.12DS3
	DS2	Extensive damage	PFA (g)	1.5	0.4	Repair		0.36DS3
	DS3	Total collapse	PFA (g)	2.2	0.4	remove	m^2	4.5
						New ceiling	m^2	66
						Coating	m^2	40.5
						paint	m^2	15

3.4 Seismic action

The GM record selection is performed using the recently developed SelEQ software [22] using a Conditional Spectrum (CS) in terms of the 5% damped spectral acceleration [23] as the target spectrum. First, the probabilistic seismic hazard analysis of the site was performed using the open source software OpenQuake [24] and the seismic hazard model developed within the SHARE project [25]. The annual seismic hazard curve H_{IM} of the benchmark site was determined at T^* for each building and is shown in Fig. 4(a).

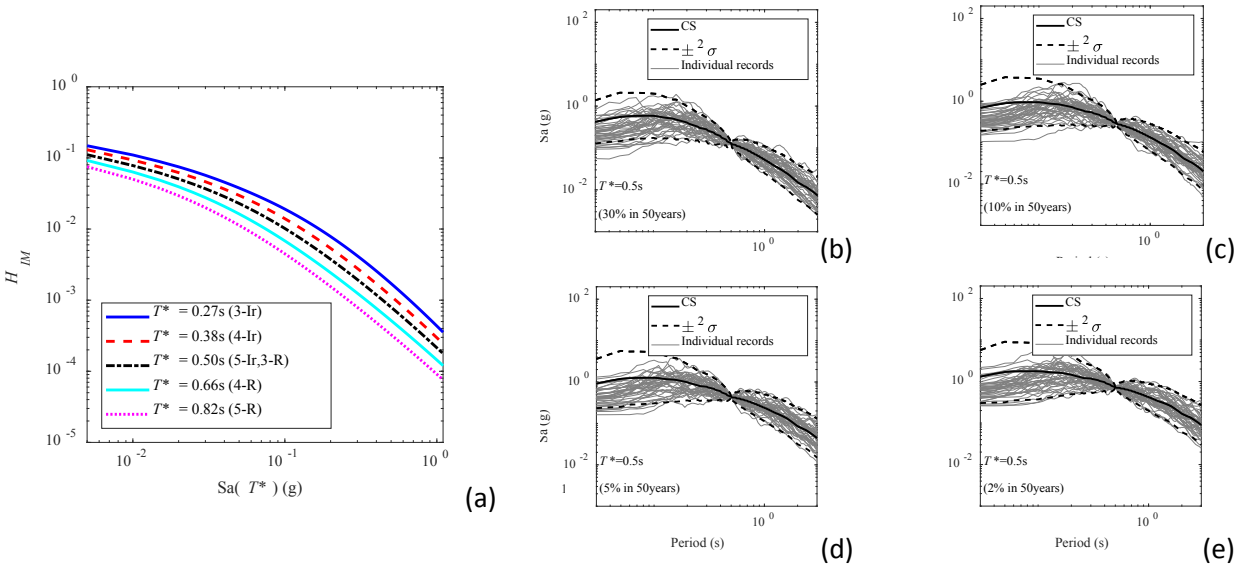

Fig. 4 – Seismic hazard curves for Lisbon and for the periods of interest (a) and the CS with the geometric mean spectra of the 40 records for each probability of exceedance, T^* = 0.50s (b)-(e).

Disaggregation of the hazard was then performed for four probabilities of exceedance, i.e. 30%, 10%, 5% and 2% in 50 years, at T^* for each building. The results were next used to build four CSs using the methodology proposed by [26]. A preliminary GM record selection was performed using the NGA-WEST2 database based on seismological and strong motion parameters, such as magnitude, epicentral distance and average shear wave velocity. Subsequently, the final selection and scaling of groups of 40 bi-directional records (for each building and for each probability of exceedance) was carried out by ensuring compatibility between the target spectrum, i.e. the CS, and the average of the geometric means of the horizontal components of all pairs. Overall, 4 groups of 40 records are selected for each building, each corresponding to a predefined probability of exceedance. See for example Fig. 4 (b) – (e) for the buildings with T^*=0.5s. Each initial group of size n = 40 is then regrouped to create ground motion groups of smaller size n = 10, 15, 20, 25, 30 and 35 using the procedure described in [16]. A total number of 100 groups are created for each new group size *n*.

3.5 Probabilistic demand model

The response of the six 3D RC building models presented in Section 3.1 is determined by performing nonlinear dynamic analysis using the GM groups defined in Section 3.4. The four GM groups selected for each building are scaled up and down to span a total of 20 intensity levels. All 40 ground motions are applied considering 12 different ASIs, ranging from 0° to 165° in steps of 15°, resulting in a total of (20 intensities×40 ground motions×12 ASIs) 9600 nonlinear 3D analyses per building (57600 total analyses). Sources of uncertainty related only to the seismic input are taken into account in the definition of the demand model, while the rest of the parameters involved, e.g. material properties, dimensions and member capacities, are considered with their mean values. More specifically, considered uncertainty stems from record-to-record variability and ASI-to-ASI variability, i.e. variability of the obtained parameters related to the finite size of GMs and of the number of ASIs used to determine the demand distributions. Although the true statistics are inherently unknown, the reference EAL considered in the current study is obtained using 40 records and 12 ASIs.

4. Results

4.1 Seismic losses of the reference case

The normalised EAL of the reference case of the six buildings, i.e. the case where all 40 GMs and all 12 ASIs are used, is shown in Fig. 5(a) as a summation of the disaggregated normalised EAL components, which are presented in the form of stacked bar plots. The total EAL values of the six buildings range from 0.10% to 0.26% of the buildings' replacement cost, in accordance with existing studies that address non-seismically designed buildings in low and moderate seismicity areas in Europe [27],[28]. It can also be seen in the same figure that the highest contribution is that of losses due to repair (i.e. the sum of losses due to the repair of structural and non-structural components), that correspond to more than 60%. Among these, losses associated to the repair of non-structural components have the largest contribution, which is in agreement with existing research results (e.g. see [18],[27]). Losses due to collapse and demolition are significantly lower and their contribution varies among the buildings.

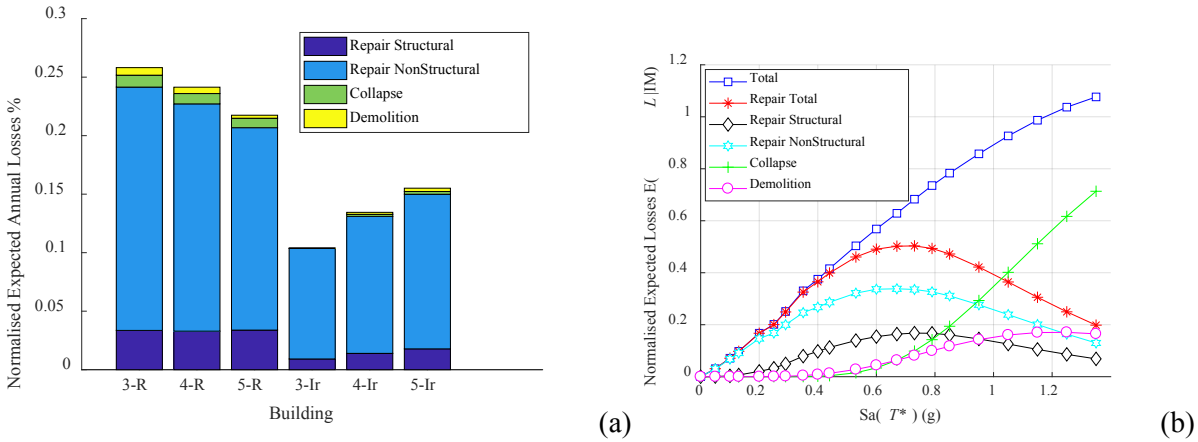

Fig. 5 – Total and disaggregated EAL of the reference cases normalised by the corresponding building replacement cost (a) and expected loss of the 3-R (a) building as a function of the ground motion intensity, normalised by the replacement cost of the building. (Reference case 40_12)

Further insights can be obtained by analysing the disaggregated losses as a function of the seismic intensity shown in Fig. 5(b), in which the normalized expected losses of the 3-R buildings for the reference case are plotted. It can be seen that losses due to the repair of structural and non-structural components outweigh the rest of the loss components for the lower and medium intensities, while losses due to collapse and demolition are the governing loss contributions for higher intensities. By considering the weighting factors assigned to each loss component by the hazard curve during the EAL calculation, expressed by Eq.

(2) (higher probabilities, thus higher weighs, for lower intensities), it can be seen that the repair losses are the main EAL. Although losses due to collapse and demolition increase with the seismic intensity, the concurrent reduction of the seismic hazard leads to a smaller overall contribution of these components in the aggregated loss, i.e. in the EAL.

4.2 Seismic losses considering the effect of the GM group size and the ASI

The effect of the GM group size and of the ASI on the EAL is examined in this section. The EAL of each building is determined for GM groups of size 10 to 40, and considers 100 groups for each size lower than 40. Furthermore, all GMs of a given group are applied along 1 to 12 ASIs resulting in 100 EAL values for each *n*_ASI combination. Fig. 6 shows the result of the six buildings (3-R, 4-R, 5-R, 5-Ir, 4-Ir, 3-Ir) for all *n* sizes and for the following *n*_ASI combinations: *n*_1, *n*_2 and *n*_12. The results for the rest of the ASIs are omitted herein due to lack of space. The bar plots in Fig. 6 correspond to the median value of the normalized total EAL for a given *n*_ASI combination (EAL_{median}), while the whiskers show the range of EAL values around the median. The normalisation is performed using the building's replacement cost.

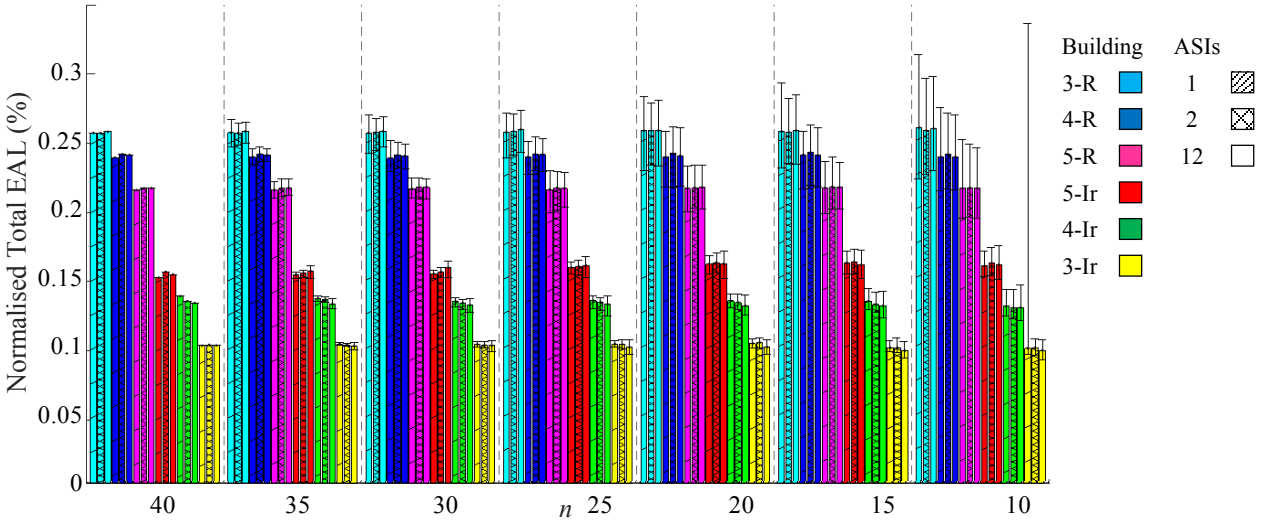

Fig. 6 – Normalised EAL of the 3-R, 4-R, 5-R, 5-Ir, 4-Ir and 3-Ir buildings for all *n*_1, *n*_2 and *n*_12 combinations

By comparing the EAL_{median} of all *n*_ASI combinations of each building to the reference EAL, i.e. the EAL_{40_12}, one of the most prominent observations that can be made is that the EAL_{median} does not experience any significant changes with the number of ASIs or with the GM group size. On the other hand, the variability of the EAL, expressed by the represented range, can be seen to change significantly depending on the GM group size. This variation can be analysed by comparing the results of the several *n*_12 combinations, in which the uncertainty related to the ASI is fully accounted for and the pure effect of the GM group size on the EAL range can be seen. As such, it is observed that by increasing the GM group size the referred range decreases. For instance, for the 3-R building, the range for the 10_12 combination is [0.0305%, 0.0374%], while for the 35_12 combination it is [0.0085, 0.0066], i.e. more than four times lower.

As opposed to the effect of the GM group size, the number of ASIs for a particular GM group size appears to have a much smaller effect on the EAL range. A slightly larger range of EAL values can be observed in cases where only 1 ASI is used for almost all GM group sizes *n* when compared to that of the *n*_12 case. Furthermore, a fairly constant range is observed for the rest of the *n*_ASI combinations, again when compared to that of the *n*_12 case (only the *n*_2 case is shown herein for brevity). Considering both the effect of the ASI and of the GM group size, when a small number of GMs is used (e.g. 10 GMs), the over- or under-estimation of the normalized EAL was found to be around 20% for most buildings studied, while extreme cases can also be found. An example of these more extreme situations comprises the 3-Ir building.

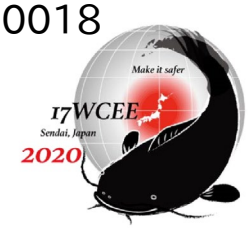

By examining the results obtained for the 10_1 combination in particular, it can be seen that a single EAL value is 340% higher than the reference value. The latter observation is an example of how a small number of observations can induce an unpredictably high variability in the outputs of a probabilistic analysis.

For the buildings analysed herein, using 25 GMs led to a 15% over- or under-estimation of the reference value, which drops to 10-12% when considering 30 GMs. Furthermore, avoiding the use of small groups of GMs (i.e. with 10 GMs or less according to the results of the examined buildings) is important to avoid the possible occurrence of extreme outliers. Using more than 1 ASI, however, does not seem to provide additional benefits for the reliable estimate of EAL, unless for cases where the GM group size is too small to provide adequate data for probabilistic analysis.

5. Conclusions

The PEER-PBEE framework was applied to analyse the effect of the GM group size and the number of ASI on the EAL of six RC buildings. An inventory of the buildings' components was defined, along with discrete damage states for each component, conditional to a response parameter, and a method of repair corresponding to a monetary value, conditional to a damage state. Additional to the loss due to repair, the loss due to collapse and demolition (in case the buildings experience excessive residual deformation) were accounted for. The building response was computed using multiple stripe analysis using hazard-compatible groups of GMs of various sizes that were applied using different number of ASIs.

The results showed that the EAL_{median} was insensitive to the GM group size and the number of ASIs. With respect to the variability, the GM group size was found to significantly influence the EAL range, leading to a reduction of the latter with its increase. The effect of the ASI on the variability, on the other hand, was shown to be much smaller and to induce only minor fluctuations on the range of the EAL. As a result, the use of only 1 ASI was considered to be adequate for the estimation of the EAL. The importance of having a large enough number of observations for probabilistic analysis was also emphasised, since extreme outliers were observed when only 10 GMs were used applied along 1 ASI. In that case, outliers were seen to disappear by increasing the number of ASIs to at least 2. Overall, for the analysed buildings, the use of 15 GMs along 1 ASI was found to be adequate for the EAL estimation. Yet, depending on the required level of precision, increasing the GM group size could be advantageous since it was shown to reduce the EAL variability. Increasing the number of ASIs, however, did not provide additional benefits.

6. Acknowledgements

Financial support of the Portuguese Foundation for Science and Technology (FCT), through the Ph.D. grant of the first author (PD/BD/113681/2015), is gratefully acknowledged. Authors also acknowledge the financial support from the Base Funding - UIDB/04708/2020 of CONSTRUCT - Instituto de I&D em Estruturas e Construções, funded by national funds through FCT/MCTES (PIDDAC).

7. References

[1] Porter KA (2003). An Overview of PEER's Performance-Based Earthquake Engineering Methodology. *9th International Conference on Applications of Statistics and Probability in Civil Engineering*. San Francisco, California.

[2] Abrahamson N, Bommer J (2005): Probability and uncertainty in seismic hazard analysis. *Earthq Spectra*, 21(2), 603-607.

[3] Haselton C, Baker J, Bozorgnia Y, Goulet C, Kalkan E, Luco N, Shantz T, Shome N, Stewart J, Tothong P, Watson-Lamprey J, Zareian F (2009): Evaluation of ground motion selection and modification methods: Predicting median interstory drift response of buildings. *Technical Report PEER 2009/01*.

[4] Franchin P, Ragni L, Rota M, Zona A (2018): Modelling uncertainties of Italian code-conforming structures for the purpose of seismic response analysis. *J Earthq Eng*, 22(sup2), 1964-1989.

[5] Lee T, Mosalam K (2006): Probabilistic seismic evaluation of reinforced concrete structural components and systems. *PEER Report 2006/04*.

[6] Haselton CB, Goulet CA, Mitrani-Reiser J, Beck JL, Deierlein GG, Porter KA and Taciroglu E (2008):. An assessment to benchmark the seismic performance of a code-conforming reinforced-concrete moment-frame building. *PEER Report 2007/1*.

[7] Calvi GM, Sullivan TJ, Welch DP (2014): A seismic performance classification framework to provide increased seismic resilience. *Perspectives on European earthquake engineering and seismology* (361-400). Springer, Cham.

[8] Cardone D, Flora, A, Picione, MDL, Martoccia A (2019): Estimating direct and indirect losses due to earthquake damage in residential RC buildings. *Soil Dynam Earthq Eng*, 126, 105801.

[9] Giannopoulos D, Vamvatsikos D (2018): Ground motion records for seismic performance assessment: To rotate or not to rotate? *Earthq Eng Struct Dyn,* 47(12), 2410-2425.

[10] Skoulidou D, Romão X (2020): The significance of considering multiple angles of seismic incidence for estimating engineering demand parameters. *Bull Earthq Eng*, 18(1), 139-163.

[11] Iervolino I (2017): Assessing uncertainty in estimation of seismic response for PBEE. *Earthq Eng Struct D,* 46(10), 1711-1723

[12] Skoulidou D, Romão X, Franchin P (2019): How is collapse risk of RC buildings affected by the angle of seismic incidence?. *Earthq Eng Struct Dyn*, 48(14), 1575-1594.

[13] Lagaros ND (2010): The impact of the earthquake incident angle on the seismic loss estimation. *Eng Struct,* 32(6), 1577-1589.

[14] Baker JW (2015): Efficient analytical fragility function fitting using dynamic structural analysis. *Earthq Spectra*, 31(1), 579–99.

[15] Ramirez CM, Miranda E (2012): Significance of residual drifts in building earthquake loss estimation. *Earthq Eng Struct Dyn*, 41(11), 1477-1493.

[16] Skoulidou D, Romão X (2019): Uncertainty quantification of fragility and risk estimates due to seismic input variability and capacity model uncertainty. *Eng Struct*, 195:425–437.

[17] McKenna F, Fenves GL (2011): Opensees 2.5.0, Computer Software. UC Berkeley, Berkeley (CA). http://opensees.berkeley.edu.

[18] Aslani H, Miranda E (2005): Probabilistic earthquake loss estimation and loss disaggregation in buildings, *Report 157* (Doctoral dissertation, Ph. D. Dissertation, John A. Blume Earthquake Engineering Center, Stanford University, United State).

[19] ASCE/SEI 41-17 (2017): *Seismic rehabilitation and retrofit of existing buildings*. American Society of Civil Engineers, Reston, VA.

[20] Cardone D, Perrone G (2017): Damage and loss assessment of pre-70 RC frame buildings with FEMA P-58. *J Earthq Eng*, 21(1), 23-61.

[21] FEMA P-58 (2012) Seismic Performance Assessment of Buildings, Volume III. Washington, D.C: Federal Emergency Management Agency.

[22] Macedo L, Castro JM (2017): SelEQ: An advanced ground motion record selection and scaling framework. *Adv Eng Softw*, 114:32–47.

[23] Baker JW (2010): Conditional mean spectrum: Tool for ground-motion selection. *J Struct Eng*, 137(3), 322-331.

[24] Pagani M, Monelli D, Weatherill G, Danciu L, Crowley H, Silva V, Simionato M (2014): OpenQuake engine: an open hazard (and risk) software for the global earthquake model. *Seismol Res Lett*, 85(3), 692–702

[25] Woessner J, Laurentiu D, Giardini D, Crowley H, Cotton F, Grünthal G, Valensine G, Arvidsson R, Basili R, Demircioglu MB, Hiemen S, Meletti C, Musson RW, Rovida AN, Sesetyan K, Stucchi M (2015): The 2013 European seismic hazard model: key components and results. *Bull Earthq Eng*, 13(12), 3553–3596.

[26] Lin T, Haselton CB, Baker JW (2013): Conditional spectrum-based ground motion selection. Part I: hazard consistency for risk-based assessments. *Earthq Eng Struct Dyn*, 42, 1847–1865.

[27] Caruso C, Bento R, Castro JM (2019): A contribution to the seismic performance and loss assessment of old RC wall-frame buildings. *Eng Struct*, 197, 109369.

[28] Sousa L, Monteiro R (2018): Seismic retrofit options for non-structural building partition walls: Impact on loss estimation and cost-benefit analysis. *Eng Struct*, 161, 8-27.

